

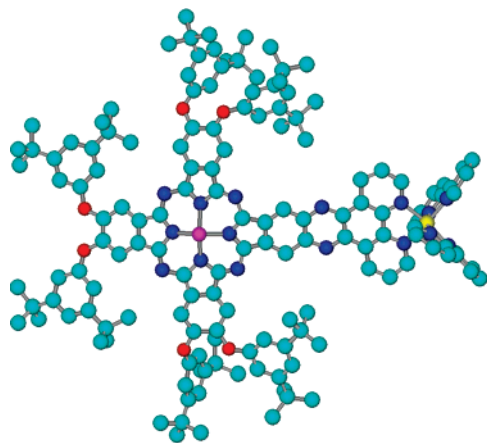
Photoinduced Energy Transfer Processes within Dyads of Metallophthalocyanines Compactly Fused to a Ruthenium(II) Polypyridine Chromophore

Marco Haas,[†] Shi-Xia Liu,^{*,†} Axel Kahnt,[‡] Claudia Leiggenger,[§] Dirk M. Guldi,^{*,‡} Andreas Hauser,[§] and Silvio Decurtins[†]

Departement für Chemie und Biochemie, Universität Bern, Freiestrasse 3, 3012 Bern, Switzerland, Institute for Physical and Theoretical Chemistry, Friedrich-Alexander-Universität Erlangen-Nürnberg, Egerlandstrasse 3, 91058 Erlangen, Germany, and Département de Chimie Physique, Université de Genève, 30 Quai Ernest-Ansermet, 1211 Genève 4, Switzerland

liu@iac.unibe.ch; dirk.guldi@chemie.uni-erlangen.de

Received June 1, 2007



An unsymmetric, peripherally octasubstituted phthalocyanine (Pc) **1**, which contains a combination of dipyrido[3,2-*f*:2',3'-*h*] quinoxaline and 3,5-di-*tert*-butylphenoxy substituents, has been obtained via a statistical condensation reaction of two corresponding phthalonitriles. Synthetic procedures for the selective metalation of the macrocyclic cavity and the periphery of **1** were developed, leading to the preparation of the key precursor metallophthalocyanines **3–5** in good yields. Two different strategies were applied to the synthesis of compact dyads MPc–Ru(II) **6–8** (M = Mg(II), Co(II), Zn(II)). Intramolecular electronic interactions in these dyads were studied by absorption, emission, and transient absorption spectroscopy. Upon photoexcitation, these dyads exhibit efficient intramolecular energy transfer from the Ru(II) chromophore to the MPc moiety.

Introduction

In recent years, the creation of multicomponent systems capable of undergoing directional electron and/or energy transfer reactions has attracted considerable attention.¹ In this context,

great efforts have been directed to the design and synthesis of discrete model systems consisting, for example, of building blocks that give rise to electron donor-acceptor interactions. For the sake of organization, such photo- and electroactive building blocks must, however, be covalently attached to each other, for which a wide range of well-defined molecular spacers have been considered.² Important variables are the nature of the donor and

[†] Universität Bern.

[‡] Friedrich-Alexander-Universität Erlangen-Nürnberg.

[§] Université de Genève.

(1) (a) LeGourriérec, D.; Anderson, M.; Davidson, J.; Mukhtar, E.; Sun, L.; Hammarström, L. *J. Phys. Chem. A* **1999**, *103*, 557. (b) Lintuluoto, J. M.; Borovkov, V. V.; Inoue, Y. *Tetrahedron Lett.* **2000**, *41*, 4781. (c) Harriman, A.; Ziessel, R. *Coord. Chem. Rev.* **1998**, *171*, 331.

(2) (a) Balzani, V.; Scandola, F. *Supramolecular Photochemistry*; Ellis Horwood: Chichester, U.K., 1991; pp 161–196, 355–394. (b) *Electron Transfer in Chemistry*; Balzani, V., Ed.; Wiley-VCH: Weinheim, 2001; Vols. I–V.

acceptor components, their relative distance, orientation, and electronic coupling, as well as aggregation induced by π - π stacking. Common to all of these variables is that they strongly affect the yields and kinetics of charge-transfer reactions in general.³ Among the many photoactive units that have been tested successfully as integrative building blocks for artificial photosynthetic systems, porphyrins and the structurally related phthalocyanines (Pcs) as well as ruthenium(II) polypyridine complexes stand out as unique components with promising absorption cross sections across the solar spectrum. Particularly important is the inherent photostability of phthalocyanines and ruthenium(II) polypyridine complexes that show little decomposition during the course of long-time photoirradiation.⁴ Most of the recent work is, however, concerned with combining these versatile chromophores with either electron-accepting fullerenes⁵ and perylene diimides⁶ or electron-donating TTF derivatives.⁷ Only a few precedents to Pcs with peripherally attached Ru(II) chromophores are known to date.⁸ For instance, Torres and co-workers^{8c} synthesized a series of $[\text{ZnPc}-\text{Ru}(\text{bpy})_3]^{2+}$ systems to study how different kinds of spacers such as amide, ethenyl,

or ethynyl modulate intramolecular electronic interactions between ZnPc and $[\text{Ru}(\text{bpy})_3]^{2+}$ moieties.

Our keen interest in the use of peripherally functionalized Pcs as ligands to form supramolecular assemblies with multi-electron redox and photoactive functions has led us to investigate the synthesis of unsymmetric, peripherally substituted Pcs.⁹ As a continuation of our previous work, we describe herein the synthetic approach toward rigidly fused $[\text{MPc}-\text{Ru}(\text{bpy})_2]^{2+}$ conjugates. In particular, $[\text{MPc}-\text{Ru}(\text{bpy})_2]^{2+}$ systems were realized by the direct coordination of an octasubstituted unsymmetric Pc that bears a single phenanthroline group at its periphery to a Ru(II) chromophore. When compared to the reported $[\text{MPc}-\text{Ru}(\text{bpy})_3]^{2+}$ conjugates, where the two building blocks are held together by flexible spacers, the rigidity and the extended π -conjugation of the present $[\text{MPc}-\text{Ru}(\text{bpy})_2]^{2+}$ conjugates provide a good geometrical control. Importantly, intramolecular electronic couplings between the individual components both in the ground state and in the excited state have been investigated by emission and transient absorption measurements.

Results and Discussion

Synthesis. Recently, we developed a synthetic procedure that affords a variety of unsymmetric Pcs with peripheral metal-binding sites in the form of pyridyl groups.⁹ In these cases, further coordination reactions with different transition metal ions were unattainable due to the conformational flexibility that arises from the 2,3-di(2-pyridyl)quinoxaline unit used as peripheral binding site. For such coordination reactions, phenanthroline derivatives offer important structural advantages, especially the rigidity that the 2,3-di(2-pyridyl)quinoxaline is lacking. Phenanthroline derivatives have indeed been extensively employed to construct elaborate transition metal complexes, which show interesting spectroscopic and redox properties as well as intercalation interactions with DNA duplexes.¹⁰ Thus, we devised and prepared an unsymmetric Pc ligand **1**, which bears one rigid phenanthroline unit, by following a synthetic procedure similar to the one previously developed.

A statistical condensation reaction of phthalonitrile precursors **A** with **B** in 1-pentanol using DBU in catalytic amounts at

(3) (a) Imahori, H.; Yamada, H.; Guldi, D. M.; Endo, Y.; Shimomura, A.; Kundu, S.; Yamada, K.; Okada, T.; Sakata, Y.; Fukuzumi, S. *Angew. Chem., Int. Ed.* **2002**, *41*, 2344. (b) Lewis, F. D.; Letsinger, R. L.; Wasielewski, M. R. *Acc. Chem. Res.* **2001**, *34*, 159. (c) Guldi, D. M.; Hirsch, A.; Scheloske, M.; Dietel, E.; Troisi, A.; Zerbetto, F.; Prato, M. *Chem.-Eur. J.* **2003**, *9*, 4968. (d) Tsue, H.; Imahori, H.; Kaneda, T.; Tanaka, Y.; Okada, T.; Tamaki, K.; Sakata, Y. *J. Am. Chem. Soc.* **2000**, *122*, 2279. (e) Kilsa, K.; Kajanus, J.; Macpherson, A. N.; Martensson, J.; Albinsson, B. *J. Am. Chem. Soc.* **2001**, *123*, 3069. (f) Fujitsuka, M.; Tsuboyana, N.; Hamasaki, R.; Ito, M.; Onodera, S.; Ito, O.; Yamamoto, Y. *J. Phys. Chem. A* **2003**, *107*, 1452. (g) Gouloumis, A.; González-Rodríguez, D.; Vázquez, P.; Torres, T.; Liu, S. G.; Echegoyen, L.; Ramey, J.; Hug, G. L.; Guldi, D. M. *J. Am. Chem. Soc.* **2006**, *126*, 12674.

(4) (a) *The Porphyrin Handbook*; Kadish, K. M., Smith, K. M., Guillard, R., Eds.; Academic Press: San Diego, CA, 2003; Vols. 15–20. (b) Imamura, T.; Fukushima, K. *Coord. Chem. Rev.* **2000**, *198*, 133. (c) de la Torre, G.; Vázquez, P.; Agulló-López, F.; Torres, T. *Chem. Rev.* **2004**, *104*, 3723. (d) Li, J.; Lindsey, J. S. *J. Org. Chem.* **1999**, *64*, 9101. (e) Zhao, Z.; Nyokong, T.; Maree, D. M. *Dalton Trans.* **2005**, 3732. (f) Zhao, Z.; Ozoemena, K. I.; Maree, D. M.; Nyokong, T. *Dalton Trans.* **2005**, 1241. (g) Tomé, J. P. C.; Pereira, A. M. V. M.; Alonso, C. M. A.; Neves, M. G. P. M. S.; Tomé, A. C.; Silva, A. M. S.; Cavaleiro, J. A. S.; Martínez-Díaz, M. V.; Torres, T.; Rahman, G. M. A.; Ramey, J.; Guldi, D. M. *Eur. J. Org. Chem.* **2006**, 257. (h) Spiccia, L.; Deacon, G. B.; Kepert, C. M. *Coord. Chem. Rev.* **2004**, *248*, 1329. (i) Ballardani, R.; Balzani, V.; Credi, A.; Gandolfi, M. T.; Venturi, M. *Acc. Chem. Res.* **2001**, *34*, 445. (j) Kon, H.; Tsuge, K.; Imamura, T.; Sasaki, Y.; Ishizaka, S.; Kitamura, N. *Inorg. Chem.* **2006**, *45*, 6875. (k) De la Torre, G.; Claessens, C. G.; Torres, T. *Chem. Commun.* **2007**, 2000.

(5) (a) Loi, M. A.; Denk, P.; Hoppe, H.; Neugebauer, H.; Winder, C.; Meissner, D.; Brabec, C.; Sariciftci, N. S.; Gouloumis, A.; Vázquez, P.; Torres, T. *J. Mater. Chem.* **2003**, *13*, 700. (b) Neugebauer, H.; Loi, M. A.; Winder, C.; Sariciftci, N. S.; Cerullo, G.; Gouloumis, A.; Vázquez, P.; Torres, T. *Sol. Energy Mater. Sol. Cells* **2004**, *83*, 201. (c) Guldi, D. M.; Gouloumis, A.; Vázquez, P.; Torres, T.; Georgakilas, V.; Prato, M. *J. Am. Chem. Soc.* **2005**, *127*, 5811. (d) de la Escosura, A.; Martínez-Díaz, M. V.; Guldi, D. M.; Torres, T. *J. Am. Chem. Soc.* **2006**, *128*, 4112. (e) Ballesteros, B.; de la Torre, G.; Torres, T.; Hug, G. L.; Rahman, G. M. A.; Guldi, D. M. *Tetrahedron* **2006**, *62*, 2097. (f) de la Escosura, A.; Martínez-Díaz, M. V.; Torres, T.; Grubbs, R. H.; Guldi, D. M.; Neugebauer, H.; Winder, C.; Drees, M.; Sariciftci, N. S. *Chem. Asian J.* **2006**, *1*–2, 148. (g) Gouloumis, A.; de la Escosura, A.; Vázquez, P.; Torres, T.; Kahnt, A.; Guldi, D. M.; Neugebauer, H.; Winder, C.; Drees, M.; Sariciftci, N. S. *Org. Lett.* **2006**, *8*, 5187. (h) Torres, T.; Gouloumis, A.; Sanchez-García, D.; Jayawickramarajah, J.; Seitz, W.; Guldi, D. M.; Sessler, J. L. *Chem. Commun.* **2007**, 292.

(6) (a) Li, X.; Sinks, L. E.; Rybtchinski, B.; Wasielewski, M. R. *J. Am. Chem. Soc.* **2004**, *126*, 10810. (b) Fukuzumi, S.; Ohkubo, K.; Ortiz, J.; Gutiérrez, A. M.; Fernández-Lázaro, F.; Sastre-Santos, Á. *Chem. Commun.* **2005**, 3814. (c) Rodríguez-Morgade, M. S.; Torres, T.; Atienza-Castellanos, C.; Guldi, D. M. *J. Am. Chem. Soc.* **2006**, *128*, 15145. (d) Jiménez, A. J.; Spänig, F.; Rodríguez-Morgade, M. S.; Ohkubo, K.; Fukuzumi, S.; Guldi, D. M.; Torres, T. *Org. Lett.* **2007**, 2481.

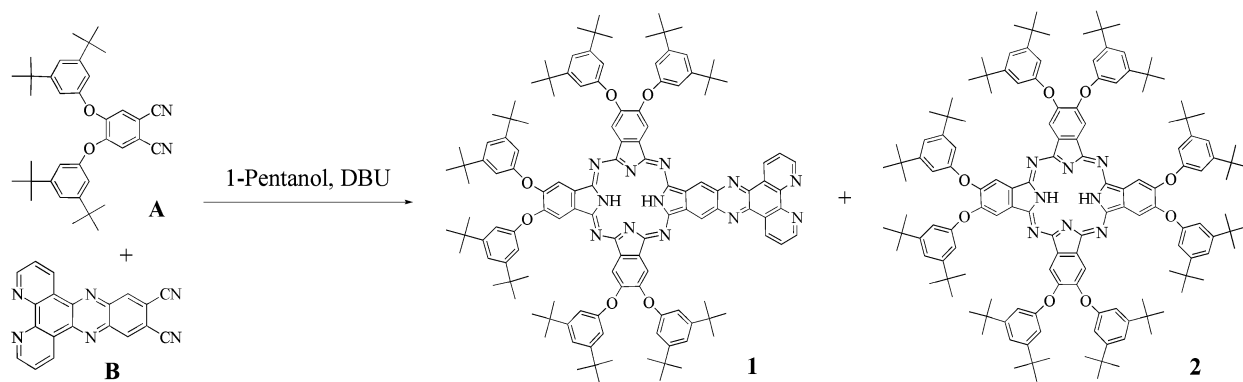
(7) (a) Loosli, C.; Jia, C.; Liu, S.-X.; Haas, M.; Dias, M.; Levillain, E.; Neels, A.; Labat, G.; Hauser, A.; Decurtins, S. *J. Org. Chem.* **2005**, *70*, 4988. (b) Sly, J.; Kasák, P.; Gomar-Nadal, E.; Rovira, C.; Górriz, L.; Thordarson, P.; Amabilino, D. B.; Rowan, A. E.; Nolte, R. J. M. *Chem. Commun.* **2005**, 1255. (c) Martínez-Díaz, M. V.; Rodríguez-Morgade, M. S.; Feiters, M. C.; van Kan, P. J. M.; Dolte, R. J. M.; Stoddart, J. F.; Torres, T. *Org. Lett.* **2000**, *2*, 1057. (d) Becher, J.; Brimert, T.; Jeppesen, J. O.; Pederson, J. Z.; Zubarev, R.; Bjørnholm, T.; Reitzel, N.; Jensen, T. R.; Kjaer, K.; Levillain, E. *Angew. Chem., Int. Ed.* **2001**, *40*, 2497. (e) Sadaïke, S.; Takimiya, K.; Aso, Y.; Otsubo, T. *Tetrahedron Lett.* **2003**, *44*, 161. (f) Li, H. C.; Jeppesen, J. O.; Levillain, E.; Becher, J. *Chem. Commun.* **2003**, 846.

(8) (a) Kimura, M.; Hamakawa, T.; Muto, T.; Hanabusa, K.; Shirai, H.; Kobayashi, N. *Tetrahedron Lett.* **1998**, *39*, 8471. (b) Kimura, M.; Hamakawa, T.; Hanabusa, K.; Shirai, H.; Kobayashi, N. *Inorg. Chem.* **2001**, *40*, 4775. (c) González-Cabello, A.; Vázquez, P.; Torres, T.; Guldi, D. M. *J. Org. Chem.* **2003**, *68*, 8635.

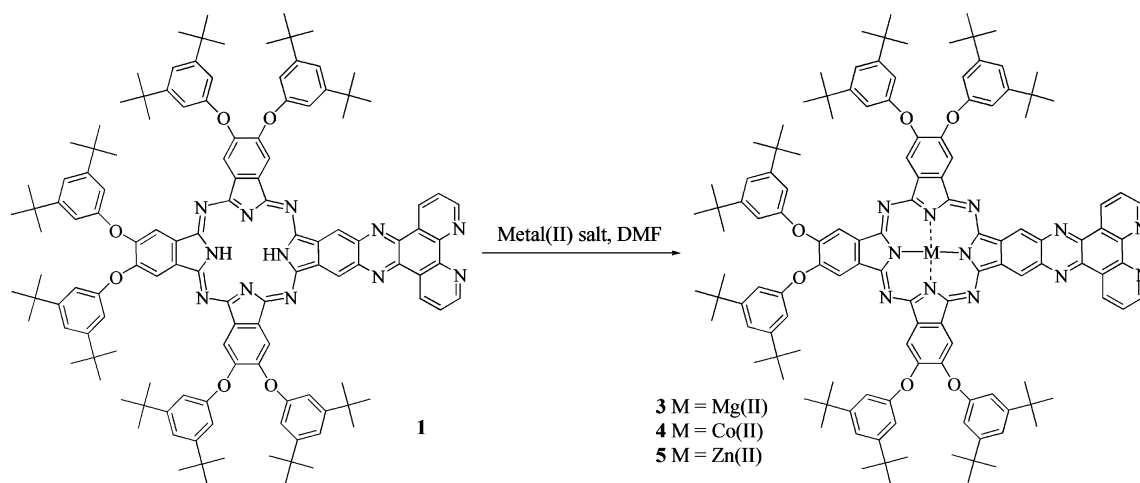
(9) Haas, M.; Liu, S.-X.; Neels, A.; Decurtins, S. *Eur. J. Org. Chem.* **2006**, 5467.

(10) (a) Rusanova, J.; Decurtins, S.; Rusanov, E.; Stoeckli-Evans, H.; Delahaye, S.; Hauser, A. *J. Chem. Soc., Dalton Trans.* **2002**, 4318. (b) Ott, S.; Faust, R. *Synthesis* **2005**, 3135. (c) Cusumano, M.; Di Pietro, M. L.; Giannetto, A. *Inorg. Chem.* **2006**, *45*, 230. (d) Liu, Y.; Chouai, A.; Degtyareva, N. N.; Lutterman, D. A.; Dunbar, K. R.; Turro, C. *J. Am. Chem. Soc.* **2005**, *127*, 10796. (e) Jia, C. Y.; Liu, S.-X.; Tanner, C.; Leiggner, C.; Neels, A.; Sanguinet, L.; Levillain, E.; Leutwyler, S.; Hauser, A.; Decurtins, S. *Chem.-Eur. J.* **2007**, *13*, 3804.

SCHEME 1. Synthetic Route to Unsymmetric Pc 1



SCHEME 2. Preparation of Metal Phthalocyanines 3–5



148 °C afforded overnight the desired AAAB type Pc **1** (Scheme 1). Generally, by varying the molar ratio of **A** and **B**, it is to some extent possible to modify the relative amounts of the individual species, which are present within the reaction mixture.¹¹ Our current investigation has shown that optimum conditions for the preferential formation of **1** involve a 4.5:1 ratio of **A** and **B**. The yields of **1** and **2** are 16% and 44%, respectively.

The choice of the phthalonitrile precursor **A** having appropriate solubilizing groups is crucial, because it has a strong impact on the separation of the desired AAAB type Pc from the mixture of different Pcs formed during the cyclotramerization reaction. For example, a green reaction mixture is obtained, when reacting **B** with 4,5-bis(*p*-pentylphenoxy)phthalonitrile, with an overall very low solubility. The UV–vis spectrum of the crude product, which reveals the characteristic Q-band features, indicates the presence of the desired AAAB type Pc. Unfortunately, the low solubility of the crude product makes separation of the desired product difficult. Exchanging the peripheral substituents, *p*-pentylphenoxy by *p*-*tert*-butylphenoxy, was expected to diminish aggregation and to enhance the solubility of the resulting Pcs. This, in turn, should favor good separation by column chromatography. However, although the crude product shows less aggregation and better solubility, only symmetric H₂Pc (AAAA)

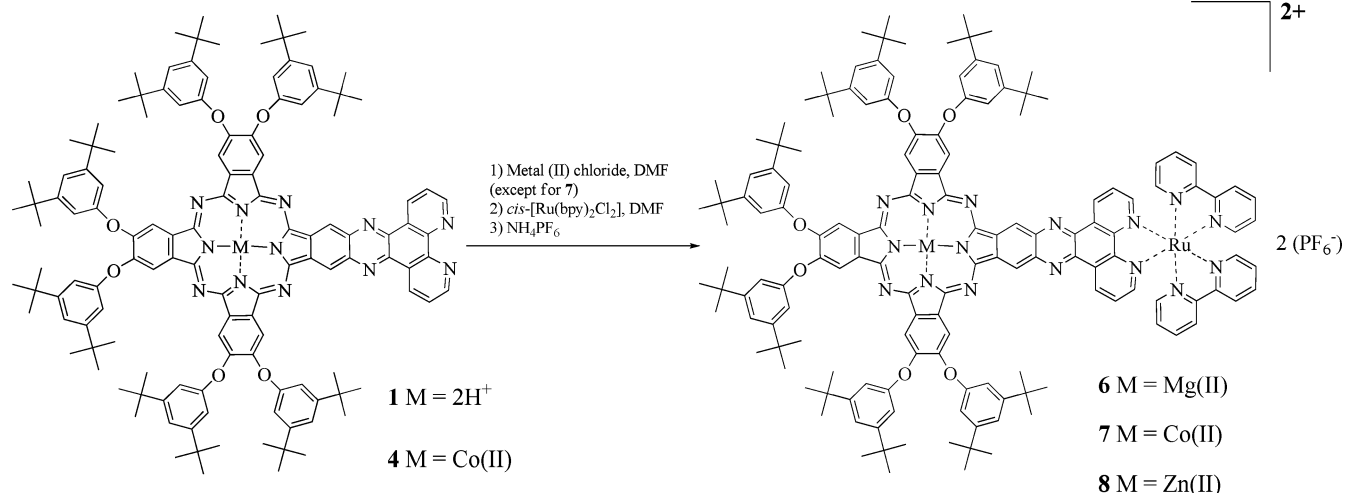
could be isolated, and the AAAB type Pc could not be eluted even if a very polar solvent mixture of CH₂Cl₂:MeOH (1:1) or acidified eluents were used. Thus, 4,5-bis(3,5-di-*tert*-butylphenoxy)phthalonitrile was finally chosen for synthesizing the target compounds.

Unsymmetric phthalocyanine **1** was reacted with various metal salts to afford the corresponding MPcs **3–5** (Scheme 2). In the case of MgPc **3**, compound **1** was reacted with a large excess of magnesium chloride hexahydrate (i.e., 30 equiv) in DMF at 150 °C overnight. These reaction conditions were, however, found to be insufficient to afford a quantitative metalation. Consequently, **3** was separated from unreacted **1** by column chromatography and isolated in 84% yield. In contrast, CoPc **4** was obtained by a reaction of **1** with 11 equiv of anhydrous cobalt(II) chloride under similar conditions. MALDI-MS and UV–vis spectra confirmed the complete metalation of **1**. Notably, the metalation of **1** with transition metal ions might generally take place at two different sites, either in the cavity of the macrocycle or at its periphery. Crossley and co-workers encountered a similar competition during the synthesis of phenanthroline functionalized zinc porphyrin systems.¹² To remove selectively the peripherally coordinated Zn(II) ions, while keeping Zn(II) bound to the macrocyclic cavity, treatment with an excess of ethylenediaminetetraacetic acid (EDTA) in boiling DMF brought the expected success.¹² A similar “EDTA strategy” for **4** to remove all non-coordinated

(11) (a) Rodríguez-Morgade, M. S.; De la Torre, G.; Torres, T. In *The Porphyrin Handbook*; Kadish, K. M., Smith, K. M., Guillard, R., Eds.; Academic Press: San Diego, CA, 2003; Vol. 15, pp 125–160. (b) Cook, M. J. *J. Chem. Rec.* **2002**, 2, 225. (c) De la Torre, G.; Torres, T. *J. Porphyrins Phthalocyanines* **2002**, 6, 274.

(12) Crossley, M. J.; Burn, P. L.; Langford, S. J.; Prashar, J. K. *J. Chem. Soc., Chem. Commun.* **1995**, 1921.

SCHEME 3. Preparation of MPc–Ru(II) Dyads 6–8



and peripherally coordinated Co(II) ions was applied, because compound **4** is not soluble enough to perform chromatographic purification. Typically, the crude product was refluxed in the presence of ethylenediaminetetraacetic acid disodium salt dehydrate for 1 day. The resulting reaction mixture was then heated in a water–methanol mixture followed by filtration to give pure **4** in 94% yield.

The aforementioned scenario for metalating **1** leads also for Zn(II) to two products, because Zn(II) fails to selectively coordinate to the Pc macrocyclic cavity. Hence, **1** was first reacted with 1.02 equiv of zinc(II) acetate dihydrate in DMF at 100 °C overnight and then with the “EDTA method” to yield pure **5** quantitatively. Additionally, it appears that high temperature and a large excess of Zn(II) facilitate the coordination reaction at the periphery as shown by MALDI-MS experiments with dithranol as a matrix. Besides the [MH]⁺ signal, a signal that could be assigned to the [M–Zn(II)–matrix]⁺ species was observed with intensities depending on the synthetic conditions.

In principle, two different strategies afforded conjugates **6** and **8**. First, it is a one-pot reaction where the preparation of unsymmetric MPcs **3** and **5** from **1**, respectively, was in situ followed by the reaction with *cis*-[Ru(bpy)₂Cl₂] (Scheme 3). Second, it is a time-consuming two-step synthesis, the initial isolation of the unsymmetric MPcs **3** and **5**, which were then reacted with *cis*-[Ru(bpy)₂Cl₂], respectively. Finally, both synthetic approaches lead to the formation of **6** and **8** in rather similar yields. The one-pot protocol involved the reaction of **1** with an excess of M(II) chloride in refluxing DMF. Upon adding the 2 equiv of *cis*-[Ru(bpy)₂Cl₂], the reaction mixture was kept at reflux for a given time period. The resulting dyad was then isolated by column chromatography. In the final purification step, the chloride anions were exchanged with hexafluorophosphate anions. In contrast, conjugate **7** could not be synthesized via the one-pot protocol. To circumvent this problem, CoPc **4** and 2 equiv of *cis*-[Ru(bpy)₂Cl₂] in refluxing DMF afforded **7** in a good yield. It is worth mentioning that the reaction of metal-free Pc **1** with *cis*-[Ru(bpy)₂Cl₂] was unsuccessful in terms of forming H₂Pc with peripherally coordinated divalent ruthenium.

Photophysics. In recent work, González-Cabello et al. reported on the photophysical investigation of several ZnPc–[Ru(bpy)₃]²⁺ conjugates, where the two building blocks were linked through a series of different covalent spacers.^{8c} Common to all of these conjugates is, regardless of the spacer, a very

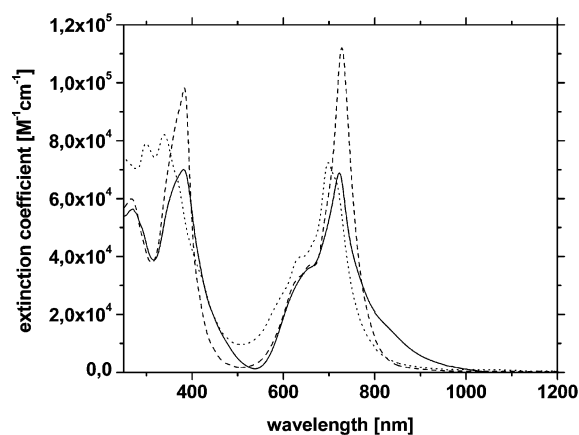


FIGURE 1. Absorption spectra of MgPc **3** (dashed spectrum), CoPc **4** (dotted spectrum), and ZnPc **5** (solid spectrum) in THF.

efficient transduction of excited-state energy that evolves between the photoexcited [Ru(bpy)₃]²⁺ and ZnPc.

The absorption spectra of the Pc references (**3**–**5**) are gathered in Figure 1. These compounds exhibit a set of Q-bands, an intense absorption maximum around 700 nm preceded by a high energetic shoulder that is typically seen around 630 nm. In addition, B-band absorptions of the Pc and π – π^* transition features arising from the dipyrido[3,2-*f*:2',3'-*h*]quinoxaline (dpq) entity and the 3,5-di-*tert*-butylphenoxy groups are observed around 370 nm as well as between 250 and 400 nm, respectively. Notably, the Q- and B-band type absorptions correspond to the spin-allowed singlet transitions S₀ → S₁ and S₀ → S₂, respectively.¹³

Figure 2 displays the analogous features for MPc–[Ru(bpy)₂]²⁺ conjugates (**6**–**8**). When compared to the Pc references **3**–**5**, an additional absorption is seen around 450 nm, which is assigned to the characteristic spin-allowed ¹MLCT transition of the Ru(II) chromophore.

Emission Measurements. ZnPc and [Ru(bpy)₂dppz]²⁺ (dppz = dipyrido[3,2-*a*:2',3'-*c*]phenazine) as reference systems both emit strongly in the monitored range, that is, between 500 and 800 nm. The [Ru(bpy)₂dppz]²⁺ complex, for example, gives rise

(13) Ishii, K.; Kobayashi, N. In *The Porphyrin Handbook*; Kadish, K. M., Smith, K. M., Guilard, R., Eds.; Academic Press: San Diego, 2003; Vol. 16, p 1.

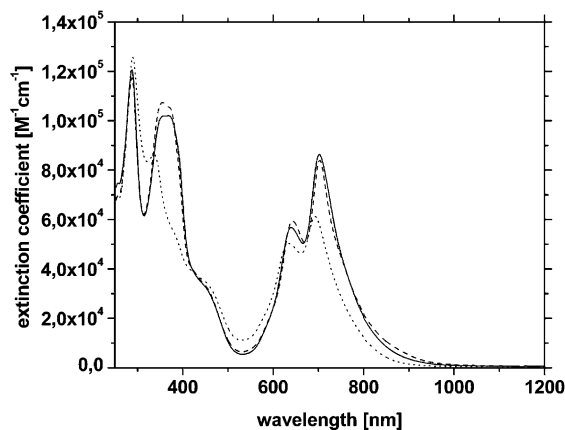


FIGURE 2. Absorption spectra of MgPc–[Ru(bpy)₂]²⁺ **6** (dashed spectrum), CoPc–[Ru(bpy)₂]²⁺ **7** (dotted spectrum), and ZnPc–[Ru(bpy)₂]²⁺ **8** (solid spectrum) in THF.

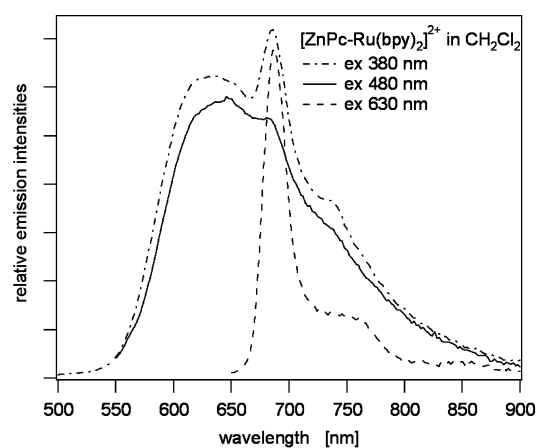


FIGURE 3. Emission spectra of the ZnPc–[Ru(bpy)₂]²⁺ conjugate (**8**) after excitation at 380 nm (dash-dotted spectrum), 480 nm (solid spectrum), and 630 nm (dashed spectrum) in CH₂Cl₂ at room temperature. The absorption at the excitation wavelengths was between 0.05 and 0.1.

to a rather broad, featureless MLCT state emission ($\lambda_{\text{max}} = 606$ nm, quantum yield: 0.044, lifetime 600 ns in de-oxygenated CH₂Cl₂ at room temperature) that has oxygen-sensitive triplet character and an excited-state energy of approximately 2.0 eV.¹⁴ In contrast, the emission from the ZnPc comes from its singlet excited state (S₁) and is sharp and strong (quantum yield: 0.3) with an excited-state energy of 1.8 eV. The corresponding ZnPc triplet excited state (T₁) lies around 1.2 eV.

When turning to the emission spectrum of the ZnPc–[Ru(bpy)₂]²⁺ conjugate **8**, two overlapping transitions are discernible with maxima at 620 and 685 nm (Figure 3). While the former bears close resemblance to the ³MLCT emission known for the related Ru(II) complex,^{10a} the latter clearly originates from the single excited-state emission of ZnPc.¹³ Implicit is that irradiation at 380 nm excites the ZnPc and likewise the Ru(II)-chromophore. To test this hypothesis, selective excitations into the ¹MLCT transition of the Ru(II) chromophore and the Q-band of ZnPc were performed. On one hand, photoexcitation at 480 nm leads nearly exclusive to the ³MLCT state emission; only residual traces of the ZnPc fluorescence are seen. On the

other hand, upon photoexcitation of the Q-band at 630 nm, only the ZnPc features are observed. Nevertheless, the emission quantum yields of the ZnPc (0.00095) and the Ru(II) chromophore (0.0015) in the ZnPc–[Ru(bpy)₂]²⁺ conjugate **8** are strongly reduced relative to those established for the corresponding references of 0.3 and 0.029, respectively. In other words, photoexcitation of either chromophore in the ZnPc–[Ru(bpy)₂]²⁺ conjugate **8** is followed by a fast excited-state deactivation. A likely rationale implies that the simultaneous quenching of both chromophores is due to an internal heavy-atom effect and a thermodynamically favored triplet–triplet energy transfer, with a driving force of approximately 0.9 eV.

The picture for the MgPc–[Ru(bpy)₂]²⁺ conjugate **6** is similar. As an example, the ³MLCT emission is quenched to 0.0055. In stark contrast, CoPc–[Ru(bpy)₂]²⁺ **7** does not exhibit luminescence due to the paramagnetic nature of the Co(II)Pc that is known to be nonluminescent.¹³

Femtosecond Transient Absorption Measurements. In summary, steady-state and time-resolved emission measurements indicate that rapid excited-state deactivation prevails in conjugates **6–8**. To shed light on the nature of the product, evolving from this intramolecular deactivation, complementary transient absorption measurements were necessary, that is, with femtosecond through to millisecond time-resolution. Following the time evolution of the characteristic singlet excited-state features of ZnPc, MgPc, etc., for instance, is a convenient mode to identify spectral features of the resulting photoproducts and to determine absolute rate constants for the intramolecular decay in conjugates **6–8**.

Differential absorption changes, following either excitation at 387 or 680 nm, of ZnPc reference **5** reveal sets of minima at 630 and 700 nm and sets of maxima at 500 and 1000 nm; see Figure 4. Hereby, the minima nicely mirror image the S₀ → S₁ absorptions seen in the ground-state absorption of ZnPc, while the maxima are part of the broad S₁ → S_n absorption features that are associated with the first excited singlet state of ZnPc. The ZnPc singlet excited state is metastable, and during the intersystem crossing process, that is, the transformation of the S₁ singlet excited state into the corresponding T₁ triplet manifold, the 500 nm maximum red shifts to 530 nm. This new transient, which has been assigned with the help of complementary nanosecond experiments to the oxygen sensitive ZnPc triplet excited state, is long-lived. A global analysis of the kinetics of the singlet excited-state decay and the triplet excited-state growth affords monoexponential lifetimes of 1195 and 897 ps for 387 and 680 nm excitation, respectively. Notable, these singlet excited lifetimes of 1050 ps are somewhat shorter than the 3100 ps typically found in simple ZnPc.¹⁵

Next, we turned to the MLCT transitions of the reference compound [Ru(bpy)₂dppz(CN)₂]²⁺ (dppz(CN)₂ = 6,7-dicyano-dipyrido[3,2-*a*:2',3'-*c*]phenazine),^{10a} which was selectively excited with laser pulses at 387 (Figure 5) or 480 nm. Here, we note the instantaneous formation of a transient species with no appreciable decay on the time scale of 3000 ps. In particular, bleaching occurs in the range of the ¹MLCT absorption ($\lambda < 525$ nm) and a transient absorption maximum occurs at 625 nm. This oxygen sensitive transient decays only on the

(14) Goze, C.; Leiggenger, C.; Liu, S.-X.; Sanguinet, L.; Levillain, E.; Hauser, A.; Decurtins, S. *ChemPhysChem* **2007**, *8*, 1504.

(15) (a) De la Escosura, A.; Martinez-Diaz, M. V.; Guldi, D. M.; Torres, T. *J. Am. Chem. Soc.* **2006**, *128*, 4112. (b) Gouloumis, A.; De la Escosura, A.; Vazquez, P.; Torres, T.; Kahnt, A.; Guldi, D. M.; Neugebauer, H.; Winder, C.; Drees, M.; Sariciftci, N. S. *Org. Lett.* **2006**, *8*, 5187.

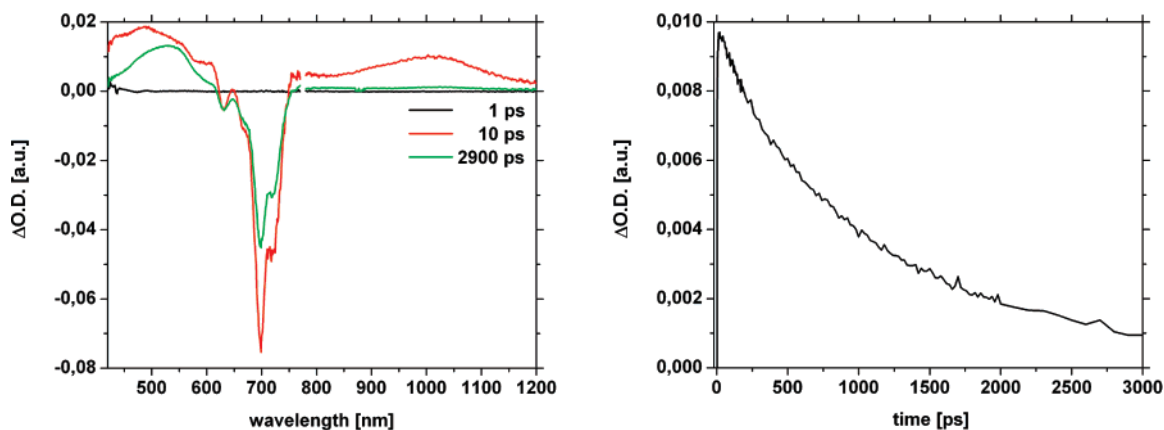


FIGURE 4. Differential absorption spectra of the ZnPc reference compound (**5**) were measured in argon saturated THF with an absorption of 0.5 at the excitation wavelength ($c \approx 40 \mu\text{M}$), excitation at 387 nm, after 1 ps (black spectrum), 10 ps (red spectrum), and 2900 ps (green spectrum) revealing the singlet–singlet and triplet–triplet excited-state features, respectively. The time profile shows the decay of the optical absorption at 1000 nm.

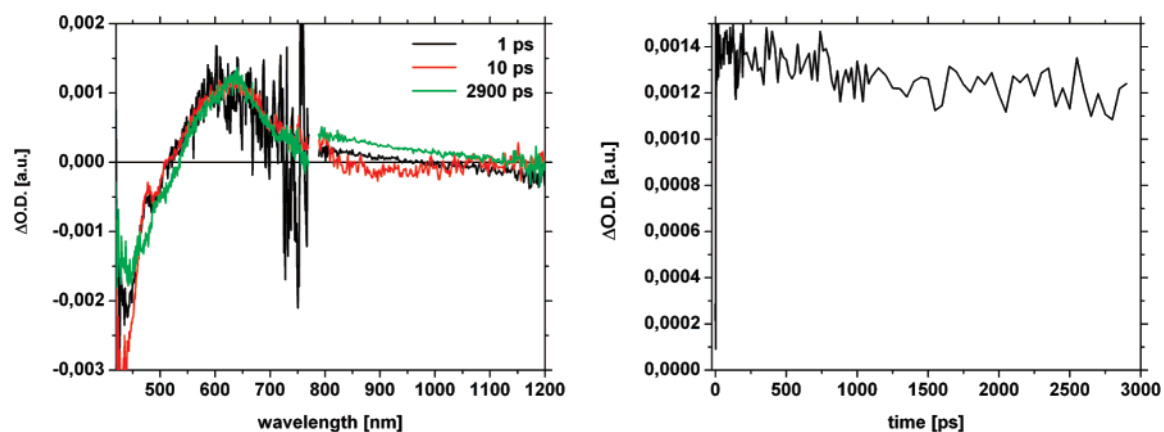


FIGURE 5. Differential absorption spectra of the $[\text{Ru}(\text{bpy})_2\text{dppz}(\text{CN})_2]^{2+}$ were measured in argon saturated THF with an absorption of 0.1 at the excitation wavelength, excitation at 387 nm, after 1 ps (black spectrum), 10 ps (red spectrum), and 2900 ps (green spectrum) revealing the triplet–triplet MLCT excited-state features. The time profile shows the change of the optical absorption at 630 nm.

nanosecond time scale. Ultrafast intersystem crossing is responsible for this observation, which converts the initially formed $^1\text{MLCT}$ state, faster than the time resolution of our instrumental setup, into the corresponding $^3\text{MLCT}$ state.¹⁶

To unravel excited-state interactions in the ZnPc– $[\text{Ru}(\text{bpy})_2]^{2+}$ conjugate (**8**), three different excitation wavelengths were used: 387 nm, to photoexcite both the Ru(II) chromophore and ZnPc; 480 nm, to photoexcite the Ru(II) chromophore only; and 680 nm, to photoexcite the ZnPc only. All of them, see Figures 6–8, give rise to the same Q-band bleaching that was already described for the ZnPc reference **5**.

Photoexcitation at 387 nm corresponds mainly to the irradiation into the $S_0 \rightarrow S_2$ transition in ZnPc. However, the emission studies have shown that the Ru(II) chromophore is also excited. Still the two transient absorption maxima, which were detected around 530 and 950 nm, correspond exclusively to that of ZnPc. Important is that the lifetime of the ZnPc singlet excited state is shorter in the ZnPc– $[\text{Ru}(\text{bpy})_2]^{2+}$ conjugate (**8**) than that in the corresponding ZnPc reference (**5**). In particular, we have determined monoexponential lifetimes of 107 and 67 ps from

the decays at 530 and 950 nm, respectively (Figure 6). This corresponds to intramolecular deactivation of $1.15 \times 10^{10} \text{ s}^{-1}$. Despite the shorter singlet excited-state lifetimes, we register at the conclusion of the decay only the ZnPc triplet excited-state features. This suggests an accelerated intersystem crossing, induced by an internal heavy atom effect due to ruthenium.

The same ZnPc singlet excited-state features were observed, but with notably lower intensities, due to lower absorption than those upon excitation at 387 nm, when photoexciting at 480 nm. For example, the differential absorption spectra with a 10 ps time delay for 387 nm excitation (Figure 6) and 480 nm excitation (Figure 7) are absolutely identical. Also, on a longer time scale, up to 3000 ps, the corresponding ZnPc triplet excited state, for which the characteristic 500 nm transient was registered, develops. What is, however, interesting is that the intensity of the 530 nm transient does not alter much during the 3000 ps time window. The only rationale that might help to explain this significant deviation from the behavior seen in the ZnPc reference (**5**) and/or the ZnPc– $[\text{Ru}(\text{bpy})_2]^{2+}$ conjugate (**8**) is the actual triplet–triplet energy transfer evolving between the $^3\text{MLCT}$ state of the Ru(II) chromophore and the ground state of ZnPc. In fact, we have used this development to successfully determine the triplet–triplet energy transfer rate as $2.5 \times 10^{12} \text{ s}^{-1}$.

(16) (a) Damrauer, N. H.; Cerullo, G.; Yeh, A.; Boussie, T. R.; Shank, C. V.; McCusker, J. K. *Science* **1997**, 275, 54. (b) Cabbizzo, A.; van Mourik, F.; Gawelda, W.; Zgrabcic, G.; Bressler, C.; Chergui, M. *Angew. Chem., Int. Ed.* **2006**, 45, 3174.

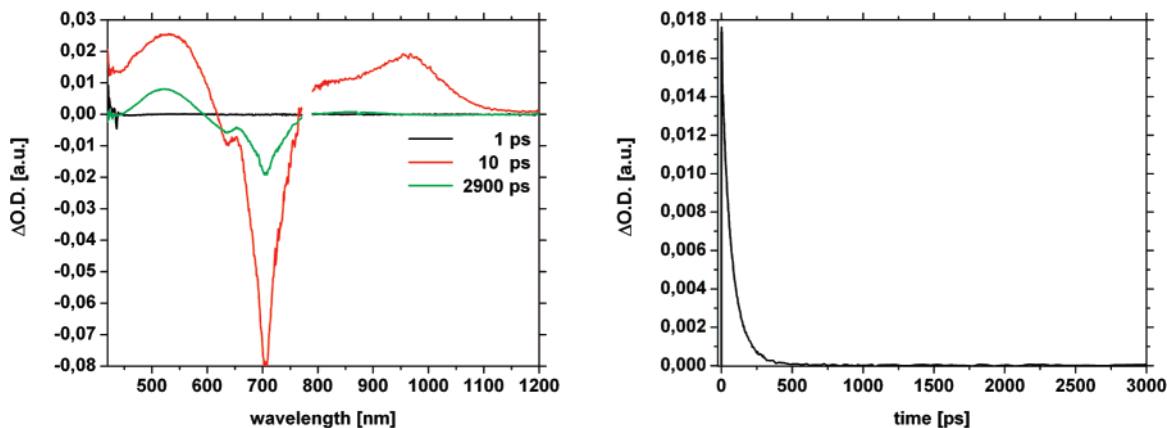


FIGURE 6. Differential absorption spectra of the ZnPc–[Ru(bpy)₂]²⁺ conjugate (**8**) were measured in argon saturated THF with an absorption of 0.5 at the excitation wavelength ($c \approx 30 \mu\text{M}$), excitation at 387 nm, after 1 ps (black spectrum), 10 ps (red spectrum), and 2900 ps (green spectrum) revealing the accelerated intersystem crossing. The time profile shows the decay of the optical absorption at 1000 nm.

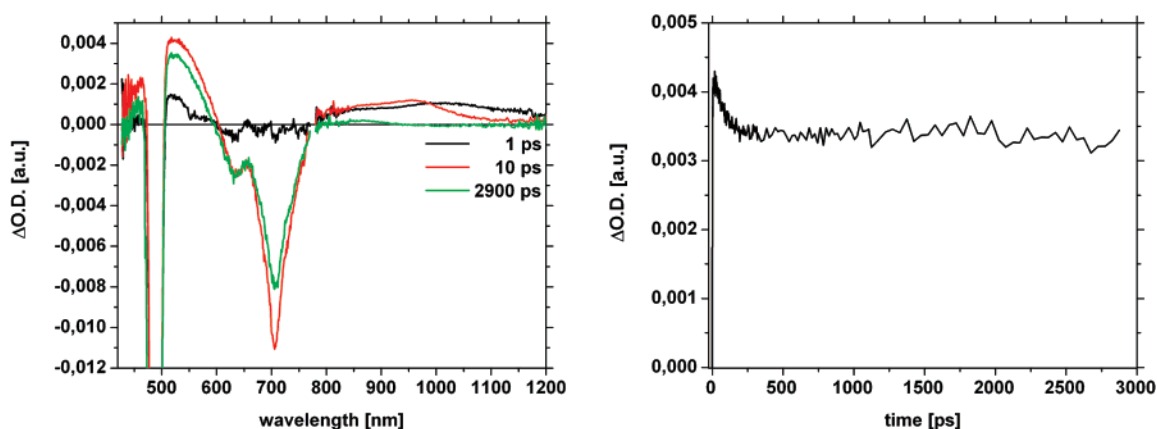


FIGURE 7. Differential absorption spectra of the ZnPc–[Ru(bpy)₂]²⁺ conjugate (**8**) were measured in argon saturated THF with an absorption of 0.1 at the excitation wavelength ($c \approx 30 \mu\text{M}$), excitation at 480 nm, after 1 ps (black spectrum), 10 ps (red spectrum), and 2900 ps (green spectrum) revealing the triplet–triplet energy transfer. The time profile shows the change of the optical absorption at 530 nm.

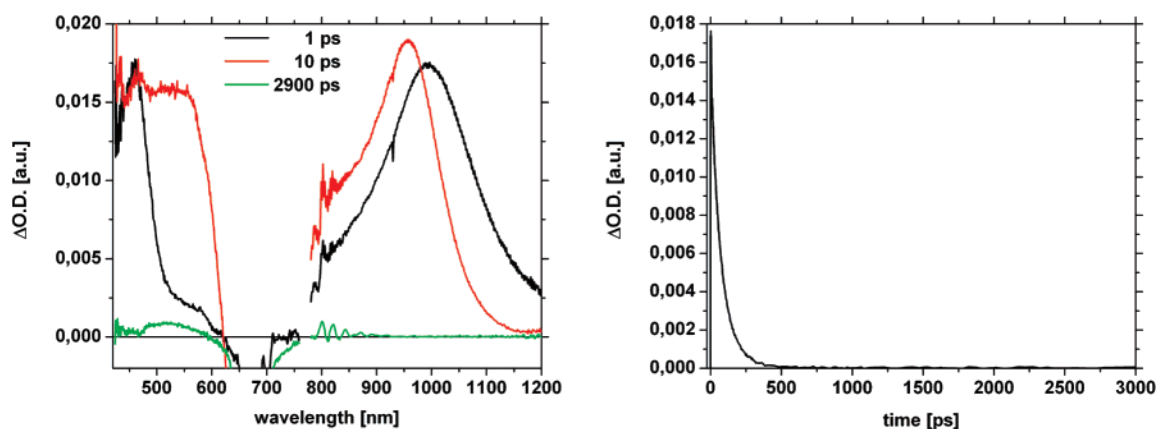


FIGURE 8. Differential absorption spectra of the ZnPc–[Ru(bpy)₂]²⁺ conjugate (**8**) were measured in argon saturated THF with an absorption of 0.4 at the excitation wavelength ($c \approx 30 \mu\text{M}$), excitation at 680 nm, after 1 ps (black spectrum), 10 ps (red spectrum), and 2900 ps (green spectrum) revealing the accelerated intersystem crossing. The time profile shows the decay of the optical absorption at 1000 nm.

Finally, photoexcitation at 680 nm was performed to test the low energetic $S_0 \rightarrow S_1$ transition in ZnPc (Figure 8). In general, the transient absorption spectra are superimposable to those noted upon 387 nm excitation. The only, but important difference between the two series of spectra is that upon photoexcitation at 680 nm, the intensity of the remaining signal

belonging to the first excited triplet (T_1) ZnPc state is much lower than in the case of the 387 nm excitation.

When turning to the MgPc reference (**3**) and the corresponding MgPc–[Ru(bpy)₂]²⁺ conjugate (**6**), we refer to the aforementioned ZnPc case. The general features in MgPc and ZnPc are nearly identical, MgPc singlet excited-state features that

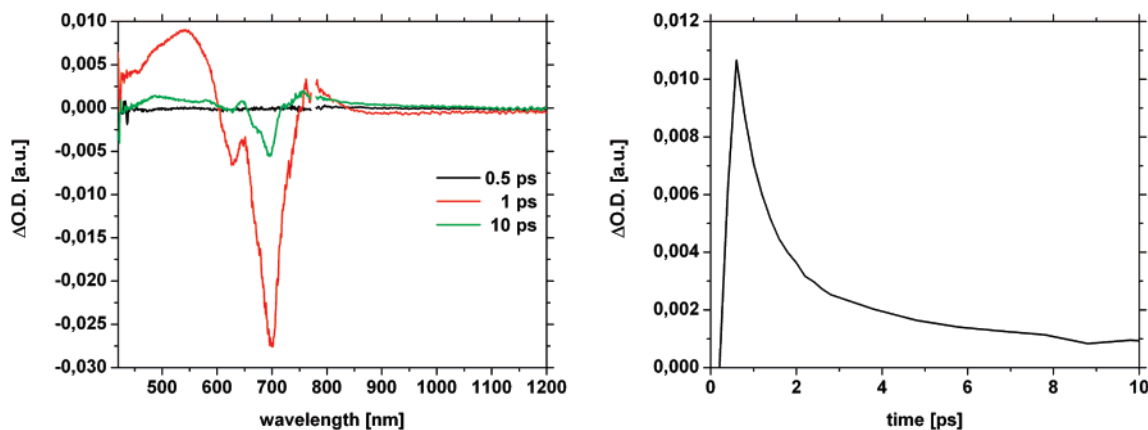


FIGURE 9. Differential absorption spectra of the CoPc–[Ru(bpy)₂]²⁺ conjugate (**7**) were measured in argon saturated THF with an absorption of 0.5 at the excitation wavelength ($c \approx 50 \mu\text{M}$), excitation at 387 nm, after 0.5 ps (black spectrum), 1 ps (red spectrum), and 10 ps (green spectrum) revealing the fast decay. The time profile shows the decay of the optical absorption at 530 nm.

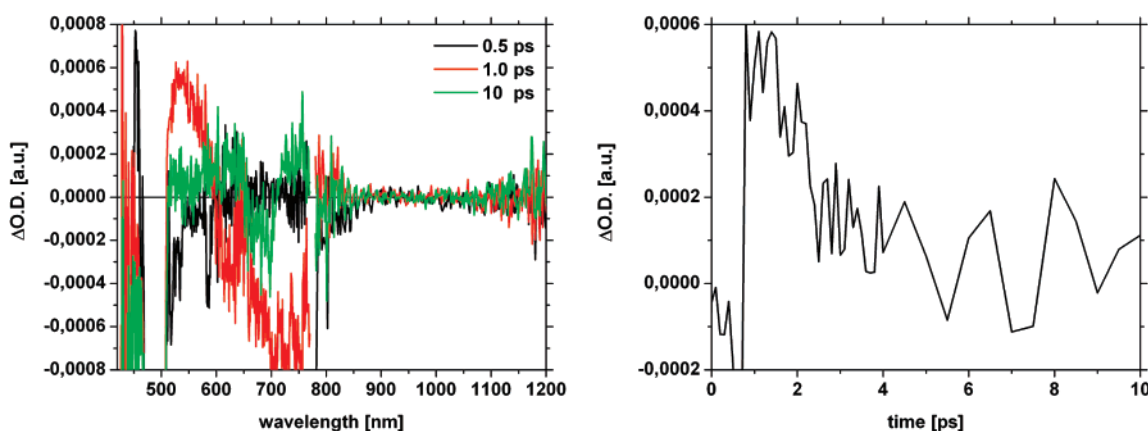


FIGURE 10. Differential absorption spectra of the CoPc–[Ru(bpy)₂]²⁺ conjugate (**7**) were measured in argon saturated THF with an absorption of 0.2 at the excitation wavelength ($c \approx 50 \mu\text{M}$), excitation at 480 nm, after 0.5 ps (black spectrum), 1 ps (red spectrum), and 10 ps (green spectrum) revealing the fast decay. The time profile shows the change of the optical absorption at 530 nm.

include maxima at 530 and 950 nm and that decay with lifetimes of 727 and 639 ps, respectively. In the corresponding MgPc–[Ru(bpy)₂]²⁺ conjugate (**6**), the lifetime is reduced to 55 ps. The corresponding rate constants are 1.4×10^9 and $1.8 \times 10^{10} \text{ s}^{-1}$ for **3** and **6**, respectively. The triplet–triplet energy transfer rate constant between the ³MLCT state of the Ru(II) chromophore and the ground state of MgPc is determined as $2 \times 10^{12} \text{ s}^{-1}$.

The general picture is, however, markedly different for the CoPc–[Ru(bpy)₂]²⁺ conjugate **7** and the CoPc reference (**4**). The decay of the excited states, as documented in Figures 9 and 10, is extremely fast in both compounds with rate constants of 10^{12} s^{-1} .

Nanosecond Transient Absorption Measurements. Photoexcitation at 355 nm of both MgPc–[Ru(bpy)₂]²⁺ and ZnPc–[Ru(bpy)₂]²⁺ conjugates (**6** and **8**) leads within the spectral window that overlaps with the femtosecond experiments, 400–900 nm, to an excellent agreement (for CoPc **7** no appreciable nanosecond transient absorption signals were obtained due to the very short lifetime of the excited singlet state). In particular, minima evolve around 370 and 700 nm, which, in line with the ground-state absorption, are assigned to bleaching of the B- and Q-bands, respectively; see Figure 11. The maxima, on the other hand, which are seen typically around 530 nm, are attributed to the $T_1 \rightarrow T_n$ absorption of ZnPc and MgPc. The underlying

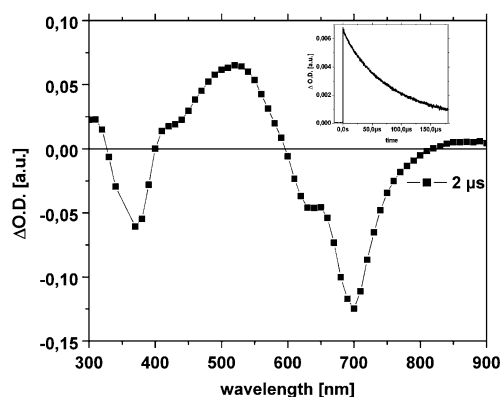


FIGURE 11. Differential absorption spectra of the ZnPc–[Ru(bpy)₂]²⁺ conjugate (**8**) were measured in THF with an absorption of 0.5 at the excitation wavelength ($c \approx 10 \mu\text{M}$), excitation at 355 nm, after 2 μs revealing the recovery of the singlet ground state. Inset time profile at 520 nm.

triplet nature, with lifetimes of 86 and 79 μs for **6** and **8**, respectively, was independently confirmed by quenching with molecular oxygen.¹⁷ The triplet quantum yields in MgPc–[Ru-

(17) Abdel-Shafi, A. A.; Wilkinson, F. *Phys. Chem. Chem. Phys.* **2002**, *4*, 248.

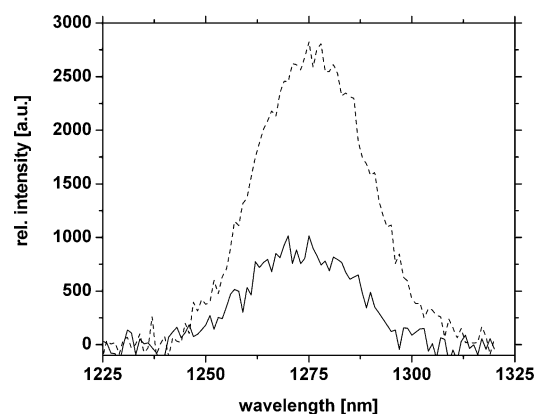


FIGURE 12. The singlet oxygen phosphorescence spectra for the ZnPc–[Ru(bpy)₂]²⁺ conjugate (**8**) (solid spectrum) and the ZnPc reference (dashed spectrum) were measured at room temperature in oxygen saturated THF with an absorption of 0.1 at the excitation wavelength of 380 nm.

(bpy)₂]²⁺ and ZnPc–[Ru(bpy)₂]²⁺ conjugates (**6** and **8**) were measured, relative to a ZnPc standard, by femtosecond transient absorption spectroscopy. Surprisingly low quantum yields of 0.18 were estimated following photoexcitation at 380 nm for both MgPc–[Ru(bpy)₂]²⁺ and ZnPc–[Ru(bpy)₂]²⁺ conjugates. An independent assessment of the triplet quantum yields was undertaken by measuring the singlet oxygen phosphorescence at 1275 nm (Figure 12). These measurements, in fact, led to the same (MgPc–[Ru(bpy)₂]²⁺, 0.18; ZnPc–[Ru(bpy)₂]²⁺, 0.17) quantum yields.

Conclusions

The present work describes two different strategies used for the synthesis of rigid MPc–Ru(II) dyad systems **6–8** via the reaction of unsymmetric dipyrido[3,2-*f*:2',3'-*h*] quinoxaline-fused Pc with [Ru(bpy)₂Cl₂]. The key step involves a statistical condensation reaction of two corresponding phthalonitriles leading to the formation of unsymmetric Pc **1**, followed by the selective metalation of the macrocyclic cavity and the periphery of **1**. Thereby, it turned out that the choice of the phthalonitrile precursor having appropriate solubilizing groups plays a crucial role in the separation of the desired 3:1 type Pc from the mixture of different Pcs formed during the cyclotetramerization reaction. A detailed study of photophysical properties of dyads **6–8**, summarized in Figure 13, demonstrates that an intramolecular energy transfer from the photoexcited Ru(II) moiety to the electron-accepting MPc unit governs their photoreactivity. The main evidence in support of the energy transfer hypothesis comes from the femtosecond transient absorption measurements. Selective excitation of the MLCT transition at 480 nm leads to the formation of the first excited triplet state of the MPc moieties in dyads **6** and **8**, which show very similar photophysical behavior. The nature of the excited triplet MPc state was confirmed by quenching with molecular oxygen in nanosecond transient absorption measurements. In addition, the bleaching of the Q-band suggests consumption of MPc as a result of converting the singlet MPc S₀ ground state to the corresponding S₁ and T₁ excited states.⁶ Excitation at 387 nm of either sample results in the rapid formation of the second excited singlet state followed by a very fast internal conversion into the first excited singlet state. Finally, intersystem crossing into the first excited triplet state was observed. Photoexcitation of the Q-band leads to the corresponding MPc S₁ states, which decay through

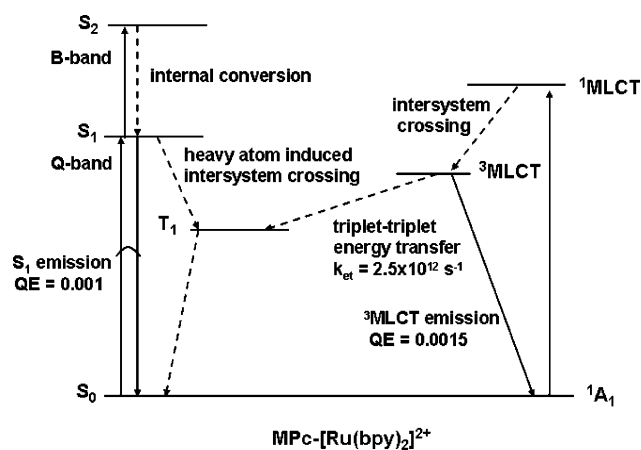


FIGURE 13. Energy level scheme for the MPc–[Ru(bpy)₂]²⁺ conjugates (M = Mg²⁺, Zn²⁺), summarizing the radiative (full lines) and nonradiative (dashed lines) processes.

intersystem crossing into the MPc T₁ states with the triplet quantum yield being qualitatively lower than that observed after excitation at 387 nm. Irradiation at 387 nm leads to higher quantum yields of the excited triplet MPc state because both subunits are excited as shown in luminescence measurements, and hence they both contribute to its formation due to an energy transfer from the Ru(II) chromophore to the MPc unit. At the same time, the lifetimes of the first excited singlet states of dyads **6** and **8** are quenched and the formation of the first excited triplet states is accelerated as compared to the corresponding Pc compound. Thus, intersystem crossing events are more probable in compounds **6** and **8** due to the heavy-atom effect exhibited by the coupled Ru(II) core. In general, dyad **7** shows the same photophysical features as **6** and **8**. The excited states were quenched by orders of magnitude, and no evidence for the formation of a first excited triplet state was found due to the paramagnetic nature of the Co(II) ion in **7**. The lifetime of the first excited singlet state is quite short, around 1.1 ps. Hence, no intersystem crossing into the first excited triplet state can take place.

It has to be emphasized that no spectral evidence for an electron transfer was found, as for instance the characteristic sharp transient absorption band of the ZnPc^{•+} at 840 nm.¹⁸ Therefore, the observed photophysical properties of dyads **6–8** are in good agreement with the results obtained by Torres et al. for similar [ZnPc–Ru(bpy)₃]²⁺ dyads, where the two chromophores are separated by different spacers.^{8c}

Experimental Section

Synthesis. 7,8-Dicyanodipyrido[3,2-*a*:2',3'-*c*]phenazine,¹⁹ 4,5-bis(3,5-di-*tert*-butylphenoxy)phthalonitrile,²⁰ and *cis*-[bis-(2,2'-bipyridine)-dichlororuthenium(II)]²¹ were synthesized according to literature procedures. All solvents and reagents were of commercial quality and used without further purification. All reactions were carried out, unless mentioned, under normal laboratory conditions in air.

(18) El-Khouly, M. E.; Ito, O.; Smith, P. M.; D'Souza, F. J. *Photochem. Photobiol., C* **2004**, *5*, 79.

(19) Rusanova, J.; Pilkington, M.; Decurtins, S. *Chem. Commun.* **2002**, 2236.

(20) Plater, M. J.; Jeremiah, A.; Bourhill, G. J. *Chem. Soc., Perkin Trans. I* **2002**, 91.

(21) Sullivan, B. P.; Salmon, D. J.; Meyer, T. J. *Inorg. Chem.* **1978**, *17*, 3334.

Phthalocyanines 1 and 2. To a mixture of 4,5-bis(3,5-di-*tert*-butylphenoxy)phthalonitrile (**A**) (2.18 g, 4.06 mmol) and 7,8-dicyanodipyrido[3,2-*a*:2',3'-*c*]phenazine (**B**) (300 mg, 903 μ mol) in 1-pentanol (20 mL) was added DBU (370 μ L, 2.47 mmol). The yellow suspension was reacted at 148 °C for 17 h under nitrogen. The green reaction mixture was then poured into a solution of CH₃-OH (50 mL) and water (30 mL). The suspension was centrifuged, washed with CH₃OH–H₂O (3:2), and the pellet was dried at 50 °C. The crude product was dissolved in CHCl₃ and subjected to column chromatography (silica). Elution with CH₂Cl₂ gave **2** (R_f = 1.0). After removal of the solvent under reduced pressure, the green precipitate was refluxed in CH₃CN, filtered hot, washed with plenty of CH₃CN, and dried at 50 °C to afford **2**. **1** was eluted with CH₂Cl₂–CH₃OH (10:1, R_f = 0.2) and purified by the same procedure as for **2**.

2,3,9,10,16,17-Hexakis(3,5-di-*tert*-butylphenoxy)-1',4',8',9'-tetraazatriphenyleno[2,3-*c*]₁-phthalocyanine (1). Green powder; yield: 274 mg (141 μ mol, 16% with respect to **B**). ¹H NMR (300 MHz, CDCl₃): δ 9.40 (s, 2H), 9.26–9.23 (m, 2H), 9.02 (s, 2H), 9.00 (s, 2H), 8.76 (s, 2H), 8.61 (s, 2H), 7.30 (t, J = 1.5 Hz, 2H), 7.25–7.18 (m, 8H), 7.15–7.13 (m, 6H), 7.02 (d, J = 1.7 Hz, 4H), 1.38 (s, 36H), 1.29 (s, 36H), 1.26 (s, 36H). IR (KBr): 3436, 2963, 1608, 1588, 1477, 1461, 1443, 1422, 1401, 1363, 1297, 1270, 1246, 1197, 1088, 1012, 960, 705 cm⁻¹. UV–vis in CHCl₃, λ_{max} (log ϵ): 292 (4.5), 358 (4.8), 412 (4.5), 625 (4.4), 673 (4.7), 694 (4.9), 739 nm (5.0). MS (MALDI, DCTB as matrix): [M + H]⁺ calcd 1944.13, found 1944.11. Anal. Calcd for C₁₂₈H₁₄₂N₁₂O₆·1.5H₂O: C, 77.98; H, 7.41; N, 8.53. Found: C, 78.21; H, 7.39; N, 8.27. TGA shows an overall weight loss of 1.4% (calcd for 1.5 molecules of water: 1.4%).

2,3,9,10,16,17,23,24-Octakis(3,5-di-*tert*-butylphenoxy)phthalocyanine (2). Grass-green powder; yield: 958 mg (446 μ mol, 44% with respect to **A**). ¹H NMR (300 MHz, CDCl₃): δ 9.33 (s, 8H), 7.53 (t, J = 1.7 Hz, 8H), 7.42 (d, J = 1.7 Hz, 16H), 1.61 (s, 144H). IR (KBr): 2963, 1608, 1588, 1461, 1440, 1423, 1395, 1316, 1298, 1270, 1198, 1087, 1012, 961, 706 cm⁻¹. UV–vis in CHCl₃, λ_{max} (log ϵ): 292 (4.7), 348 (4.8), 396 (4.6), 608 (4.5), 641 (4.6), 670 (5.1), 705 nm (5.2). MS (MALDI, dithranol as matrix): [M + H]⁺ calcd 2148.38, found 2148.38. Anal. Calcd for C₁₄₄H₁₇₈N₈O₈: C, 80.48; H, 8.35; N, 5.21. Found: C, 80.82; H, 8.58; N, 5.07. TGA shows no loss of solvent.

[2,3,9,10,16,17-Hexakis(3,5-di-*tert*-butylphenoxy)-1',4',8',9'-tetraazatriphenyleno[2,3-*c*]₁]phthalocyaninato]magnesium(II) (3). A mixture of **1** (34 mg, 17.5 μ mol) and MgCl₂·6H₂O (106 mg, 521 μ mol) in DMF (5 mL) was heated at 150 °C overnight under nitrogen. Afterward, the solvent was removed and the blue crude product was dissolved in CHCl₃ and chromatographed through a neutral alumina column eluting with CH₂Cl₂–CH₃OH (100:1). After the solvents were removed, the product was heated in CH₃OH–H₂O (1:1; 100 mL) at 70 °C. The blue suspension was then filtered, washed with plenty of CH₃OH, and dried at 80 °C to yield **3** as a blue solid (29 mg, 14.7 μ mol, 84%).

IR (KBr): 3437, 2962, 1608, 1587, 1481, 1447, 1422, 1400, 1353, 1297, 1267, 1196, 1087, 1035, 961 cm⁻¹. UV–vis in CHCl₃, λ_{max} (log ϵ): 270 (4.9), 380 (5.0), 641 (4.5), 714 (5.0), 727 nm (5.0). MS (MALDI, dithranol as matrix): [M + H]⁺ calcd 1966.09, found 1966.10. Anal. Calcd for C₁₂₈H₁₄₀N₁₂O₆Mg·4.5H₂O: C, 75.07; H, 7.33; N, 8.21. Found: C, 74.70; H, 7.10; N, 7.93. TGA shows an overall weight loss of 4.1% (calcd for 4.5 molecules of water: 4.0%).

[2,3,9,10,16,17-Hexakis(3,5-di-*tert*-butylphenoxy)-1',4',8',9'-tetraazatriphenyleno[2,3-*c*]₁]phthalocyaninato]cobalt(II) (4). A mixture of **1** (60 mg, 31 μ mol) and CoCl₂ (44 mg, 339 μ mol) in DMF (6 mL) was heated at 150 °C for 16 h under nitrogen. Next, ethylenediaminetetraacetic acid disodium salt dihydrate (504 mg, 1.35 mmol) was added to the blue reaction mixture, which was kept at 150 °C for a further day. The reaction mixture was then poured into CH₃OH–H₂O (1:1; 100 mL) and heated at 75 °C for

6 h. The precipitate was filtered off when hot, washed with plenty of H₂O, and dried at 80 °C to yield **4** as a blue solid (58 mg, 29 μ mol, 94%).

IR (KBr): 3435, 2963, 1608, 1588, 1478, 1459, 1420, 1351, 1297, 1272, 1197, 1094, 1051, 961 cm⁻¹. UV–vis in CHCl₃, λ_{max} (log ϵ): 309 (4.8), 338 (4.8), 629 (4.4), 698 nm (4.9). MS (MALDI, dithranol as matrix): [M + H]⁺ calcd 2001.04, found 2001.04. Anal. Calcd for C₁₂₈H₁₄₀N₁₂O₆Co·3.5H₂O: C, 74.47; H, 7.18; N, 8.14. Found: C, 74.44; H, 6.97; N, 8.20. TGA shows an overall weight loss of 2.9% (calcd for 3.5 molecules of water: 3.1%).

[2,3,9,10,16,17-Hexakis(3,5-di-*tert*-butylphenoxy)-1',4',8',9'-tetraazatriphenyleno[2,3-*c*]₁]phthalocyaninato]zinc(II) (5). A mixture of **1** (200 mg, 103 μ mol) and Zn(OAc)₂·2H₂O (23 mg, 105 μ mol) in DMF (20 mL) was heated at 100 °C overnight under nitrogen. Next, ethylenediaminetetraacetic acid disodium salt dihydrate (50 mg, 134 μ mol) was added. The blue reaction mixture was kept at 100 °C for another 8 h. Upon the addition of CH₃-OH–H₂O (1:1; 150 mL), the mixture was heated at 75 °C for 6 h. The precipitate was filtered off when hot, washed with plenty of boiling H₂O, and dried at 80 °C to yield **5** as a blue solid (203 mg, 101 μ mol, 98%).

IR (KBr): 3444, 2964, 1609, 1587, 1448, 1423, 1402, 1353, 1297, 1268, 1197, 1092, 1036, 962 cm⁻¹. UV–vis in CHCl₃, λ_{max} (log ϵ): 377 (4.3), 638 (3.9), 708 (4.3), 726 nm (4.3). MS (MALDI, dithranol as matrix): [M + H]⁺ calcd 2006.04, found 2006.04. Anal. Calcd for C₁₂₈H₁₄₀N₁₂O₆Zn·1.2H₂O: C, 75.75; H, 7.07; N, 8.28. Found: C, 75.62; H, 7.12; N, 8.22. TGA shows an overall weight loss of 1.0% (calcd for 1.2 molecules of water: 1.1%).

Bis(2,2'-bipyridine){[2,3,9,10,16,17-hexakis(3,5-di-*tert*-butylphenoxy)-1',4',8',9'-tetra-azatriphenyleno[2,3-*c*]₁]phthalocyaninato]magnesium(II)}ruthenium(II) Dihexafluorophosphate (6). Magnesium chloride hexahydrate (62 mg, 305 μ mol) and **1** (30 mg, 15 μ mol) in DMF (3 mL) were refluxed at 160 °C overnight under nitrogen. Next, [Ru(bpy)₂Cl₂]₂·2H₂O (16 mg, 31 μ mol) was added, and the reaction mixture was stirred at 160 °C for an additional 10 h. DMF was then removed by rotary evaporation, and the crude product was dissolved in CHCl₃. The resulting green solution was subjected to a neutral alumina column. A blue and a purple fraction were removed by eluting with CH₂Cl₂–CH₃OH (20:1). The desired product was isolated using CH₂Cl₂–CH₃OH (15:1, R_f = 0.4) as eluent. After the solvents were removed, the green solid was dissolved in a minimum amount of EtOH and filtered. An aqueous solution of NH₄PF₆ (120 mg, 736 μ mol) was added to the stirred green solution. The resulting precipitate was then filtered and washed with plenty of H₂O. The green solid was collected and dried at 80 °C (28 mg, 11 μ mol, 68%).

IR (KBr): 3436, 2962, 1607, 1586, 1447, 1422, 1401, 1297, 1268, 1196, 1088, 1034, 960, 845, 558 cm⁻¹. UV–vis in CHCl₃, λ_{max} (log ϵ): 286 (4.9), 371 (4.8), 640 (4.5), 704 nm (4.6). MS (ESI, CH₃OH): [M – 2PF₆]²⁺ calcd 1189.57, found 1189.56. Anal. Calcd for C₁₄₈H₁₅₆N₁₆O₆F₁₂MgP₂Ru·5H₂O: C, 64.40; H, 6.06; N, 8.12. Found: C, 64.56; H, 5.91; N, 7.88. TGA shows an overall weight loss of 3.4% (calcd for 5 molecules of water: 3.3%).

Bis(2,2'-bipyridine){[2,3,9,10,16,17-hexakis(3,5-di-*tert*-butylphenoxy)-1',4',8',9'-tetra-azatriphenyleno[2,3-*c*]₁]phthalocyaninato]cobalt(II)}ruthenium(II) Dihexafluorophosphate (7). A mixture of **4** (40 mg, 20 μ mol) and *cis*-[Ru(bpy)₂Cl₂]₂·2H₂O (21 mg, 40 μ mol) in DMF (3 mL) was refluxed at 160 °C for 20 h under nitrogen. Next, DMF was removed under reduced pressure, and the bluish green solid was dissolved in a minimum amount of CHCl₃. The solution was chromatographed through a neutral alumina column. The eluent, CH₂Cl₂–CH₃OH, was changed from an initial ratio of 25:1 to 15:1 (R_f = 0.3). After removal of solvents from the bluish green fractions, the residue was dissolved in a minimum amount of ethanol and filtered. An aqueous solution of NH₄PF₆ (100 mg, 613 μ mol) was added to the green solution and stirred at rt until precipitation was complete. After 50 mL of water was added, the green suspension was filtered, washed with plenty of water, and dried at 80 °C (34 mg, 13 μ mol, 63%).

IR (KBr): 3435, 2956, 1607, 1586, 1448, 1416, 1396, 1350, 1296, 1272, 1196, 1097, 1052, 960, 843, 558 cm^{-1} . UV–vis in CHCl_3 , λ_{max} (log ϵ): 290 (5.0), 336 (4.9), 630 (4.6), 693 nm (4.7). MS (ESI, CH_3OH): $[\text{M} - 2\text{PF}_6]^{2+}$ calcd 1207.04, found 1207.04. Anal. Calcd for $\text{C}_{148}\text{H}_{156}\text{N}_{16}\text{O}_6\text{CoF}_{12}\text{P}_2\text{Ru}\cdot 3\text{H}_2\text{O}$: C, 64.43; H, 5.92; N, 8.12. Found: C, 64.44; H, 5.92; N, 8.06. TGA shows an overall weight loss of 2.1% (calcd for 3 molecules of water: 2.0%).

Bis(2,2'-bipyridine){[2,3,9,10,16,17-hexakis(3,5-di-*tert*-butylphenoxy)-1',4',8',9'-tetra-azatriphenyleno[2,3-*c*₁]phthalocyaninato]-zinc(II)}ruthenium(II) Dihexafluorophosphate (8). A mixture of **1** (66 mg, 34 μmol) and ZnCl_2 (19 mg, 139 μmol) in DMF (4 mL) was heated at 160 $^\circ\text{C}$ for 3 h under nitrogen. Upon the addition of $[\text{Ru}(\text{bpy})_2\text{Cl}_2]\cdot 2\text{H}_2\text{O}$ (35 mg, 67 μmol), the blue reaction mixture was refluxed for another 4 h. Next, DMF was removed under reduced pressure, and the residue was dissolved in a minimum amount of CHCl_3 . The chromatographic procedure and the anion exchange process were carried out as described for **6**. The green solid was collected and dried at 80 $^\circ\text{C}$ (53 mg, 20 μmol , 58%).

IR (KBr): 2962, 1607, 1585, 1447, 1422, 1403, 1297, 1269, 1196, 1093, 1035, 961, 845, 558 cm^{-1} . UV–vis in CHCl_3 , λ_{max}

(log ϵ): 287 (5.0), 368 (4.9), 637 (4.6), 701 nm (4.8). MS (ESI, CH_3OH): $[\text{M} - 2\text{PF}_6]^{2+}$ calcd 1209.54, found 1209.54. Anal. Calcd for $\text{C}_{148}\text{H}_{156}\text{N}_{16}\text{O}_6\text{F}_{12}\text{P}_2\text{RuZn}\cdot 4\text{H}_2\text{O}$: C, 63.86; H, 5.94; N, 8.05. Found: C, 64.18; H, 5.92; N, 7.80. TGA shows an overall weight loss of 3.0% (calcd for 4 molecules of water: 2.6%).

Acknowledgment. Financial support from the Swiss National Science Foundation (grant no. 200020-116003 and COST Action D31), the ESF program–SONS (NANOSYN) as well as from SFB 583, DFG (GU 517/4-1), FCI and the Office of Basic Energy Sciences of the U.S. Department of Energy is greatly appreciated. We also thank Fredy Nydegger (University of Fribourg) for mass spectra.

Supporting Information Available: General experimental methods and ^1H spectra for compounds **1** and **2**. This material is available free of charge via the Internet at <http://pubs.acs.org>.

JO0710477